JOURNAL OF GEOPHYSICAL RESEARCH, VOL. 106, NO. A12, PAGES 29,037–29,050, DECEMBER 1, 2001

A substorm onset signature at the auroral zone as observed with SuperDARN and equatorial magnetometers

O. Saka,[1,2] T. Kitamura,[2] H. Tachihara,[2] M. Shinohara,[2] N. B. Trivedi,[3] N. Sato,[4] J. M. Ruohoniemi,[5] and R. A. Greenwald[5]

Abstract. Ionospheric convection enhancement with high westward velocities exceeding 1500 m s^{-1} was observed in association with the particle injection event by SuperDARN in the dusk sector of the auroral zone. Such a convection enhancement could be attributable to the enhanced sunward plasma flows in the dusk sector of the magnetosphere. At the dip equator a ground Pi2 onset was found to occur in association with these convection transients. The onset of the Pi2 lagged behind the convection enhancement by 4–11 min. It is argued that the convection transient could be the earliest indicator of the substorm onset among energetic particle injection, low-latitude Pi2 onset, and, perhaps, the auroral breakup.

1. Introduction

Pi2 pulsations have been considered as a wave signal transmitted to the ground from the midnight sector where the substorm expansion takes place [*Saito*, 1969; *Jacobs*, 1970; *Lanzerotti and Fukunishi*, 1974; *Southwood and Stuart*, 1980; *McPherron*, 1980]. The substorm signatures in the magnetic field and energetic particle disturbances have been examined in reference to these ground Pi2s [*Sakurai and McPherron*, 1983; *Yeoman et al.*, 1994; *Olson*, 1999; and references therein]. Recently, an examination of the Pi2 onset at geosynchronous altitudes revealed that the Pi2 was triggered by the transient response of the geomagnetic fields to the increased plasma pressures in the inner magnetosphere at the substorm onset [*Saka et al.*, 2000a]. A question arose, however, as to whether the substorm onset indicators, such as low-latitude Pi2, auroral breakup, and dispersionless energetic particle injection, appear in the midnight sector coincidentally within a timescale of minutes [*Liou et al.*, 1999].

The effect of the ring currents in the inner magnetosphere [*Akasofu and Meng*, 1968; *Onwumechili et al.*, 1973] and the thermodynamic effect from the disturbed neutral wind in the ionosphere [*Blanc and Richmond*, 1980] were other components of the magnetospheric effect that can be seen at the equator. Although the Earth is often shielded electrically against the primary electric fields in the solar wind by the space charges built up in the magnetosphere (Alfven layer) [e.g., *Nishida*, 1978], the secondary electric fields in the inner magnetosphere that emerged from the shielding process often penetrate to the equator [*Senior and Blanc*, 1984].

In this report we examine a global response of the magnetosphere as observed by SuperDARN and equatorial magnetometers at substorm onset. Instead of the direct penetration of the electric fields, a Pi2 pulsation was recorded at the equator when a substorm-associated convection enhancement was seen to occur in the dusk sector of the auroral region. These ground substorm signatures did not occur coincidentally.

2. Observations

2.1. September 25, 1994, Event

Figures 1a and 1b depict a 5-day plot of the energetic particle differential flux (proton for P1 through P4 and electron for E1 through E4) from Los Alamos National Laboratory (LANL) geosynchronous satellites 1984-129 (8.4° in geographic longitudes) and 1987-097 (103.7° in geographic longitudes). The particle injection event that occurred on September 25, 1994, was observed by the proton detector on board 1984-129 at the premidnight sector, 1904 LT, as well as by the electron detector on board 1984-097 at the postmidnight sector, 0122 LT. At these satellite locations the injection onset was seen to occur at 1830 UT, as marked by the vertical bar. Figures 1c and 1d depict ground magnetometer data from Christmas Island (CRI; 3.09°N, 273.49° in geomagnetic coordinates; 2.00°N, −157.5° in geographic coordinates) and the *Dst* index. It is apparent that a diurnal change of the geomagnetic fields at CRI, which was then at the dayside sector (0800 LT), was greatly modified after the injection by the effect of the westward flowing ring currents that were enhanced by these injection activities in the nightside magnetosphere.

SuperDARN HF radar beams from Saskatoon (T), Kapuskasing (K), Goose Bay (G), and Stokkseyri (W) covered the afternoon sector of the auroral zone during the injection onset. Echoes were returned mostly from the afternoon sector. In Figure 2 we look at the injection event with an enlarged timescale by examining the maximum flow velocity in the radar field of view and the ground Pi2 signature. Among multiple Pi2 onsets, as can be seen during the first 1-hour interval after the injection, the first two Pi2 onsets, as marked by the vertical bars, are clearly identified as being accompanied by the corresponding convection enhancement and the concurrent particle injection. Below, we will examine the initial Pi2 onset that

[1]Department of Physics, Kurume National College of Technology, Kurume, Japan.
[2]Department of Earth and Planetary Sciences, Kyushu University, Fukuoka, Japan.
[3]Instituto Nacional de Pesquisas Espacias, Sao Jose dos Campos, Spain.
[4]National Institute of Polar Research, Tokyo, Japan.
[5]Applied Physics Laboratory, Johns Hopkins University, Laurel, Maryland, USA.

Paper number 2001JA900091.
0148-0227/01/2001JA900091$09.00

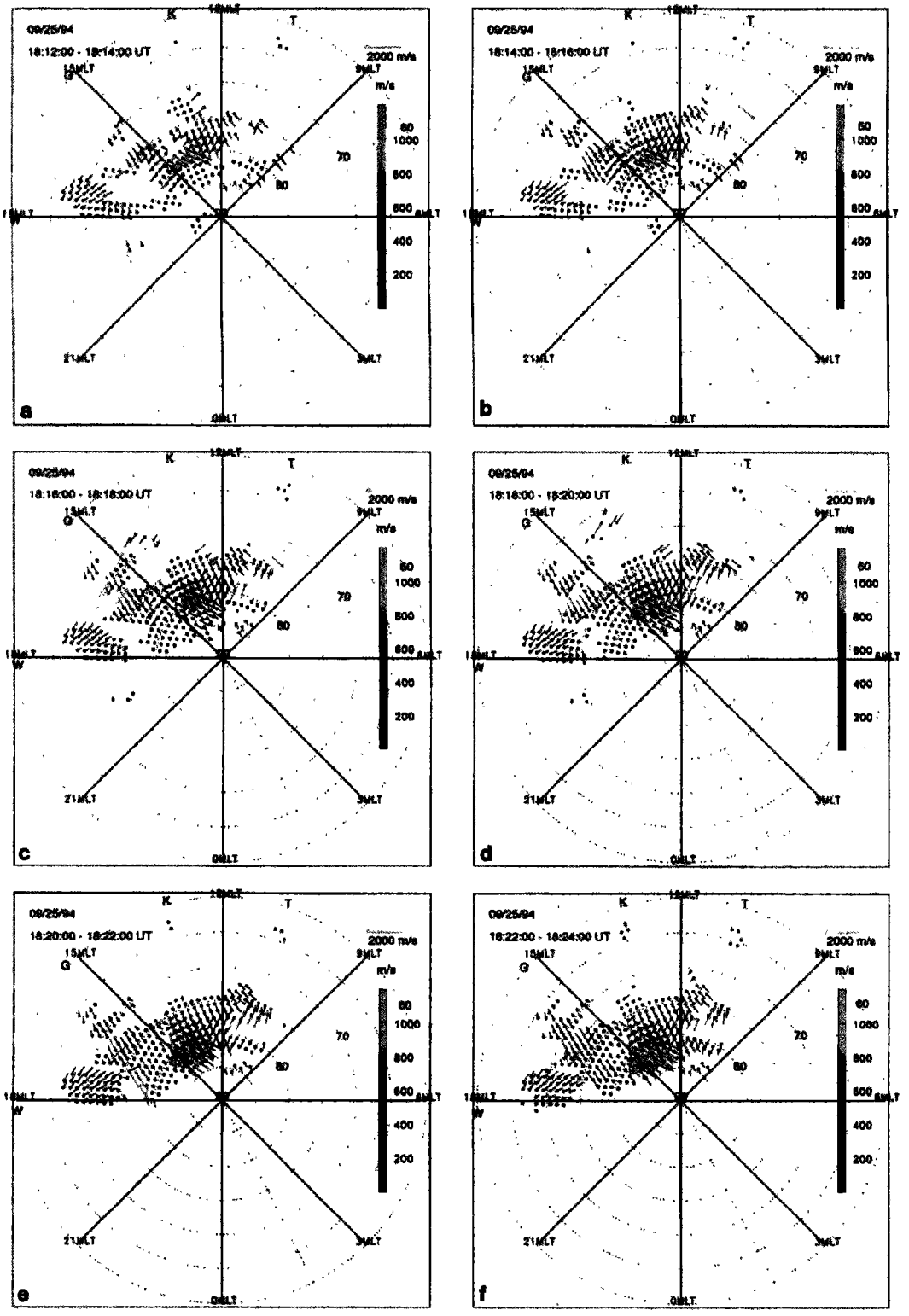

Plate 1. Plot of the averaged line-of-sight velocity values obtained from the SuperDARN radars on September 25, 1994; (a) 1812:00–1814:00 UT, (b) 1814:00–1816:00 UT, (c) 1816:00–1818:00 UT, (d) 1818:00–1820:00 UT, (e) 1820:00–1822:00 UT, (f) 1822:00–1824:00 UT, (g) 1824:00–1826:00 UT, (h) 1826:00–1828:00 UT, (i) 1828:00–1830:00 UT, (j) 1830:00–1832:00 UT, (k) 1832:00–1834:00 UT, (l) 1834:00–1836:00 UT, (m) 1836:00–1838:00 UT, (n) 1838:00–1840:00 UT, (o) 1840:00–1842:00 UT, (p) 1842:00–1844:00 UT, (q) 1844:00–1846:00 UT, (r) 1846:00–1848:00 UT. The longitude positions (in geomagnetic coordinates) of the contributing radars are indicated by the letters along the 60°N contour: T, Saskatoon; K, Kapuskasing; G, Goose Bay; W, Stokkseyri.

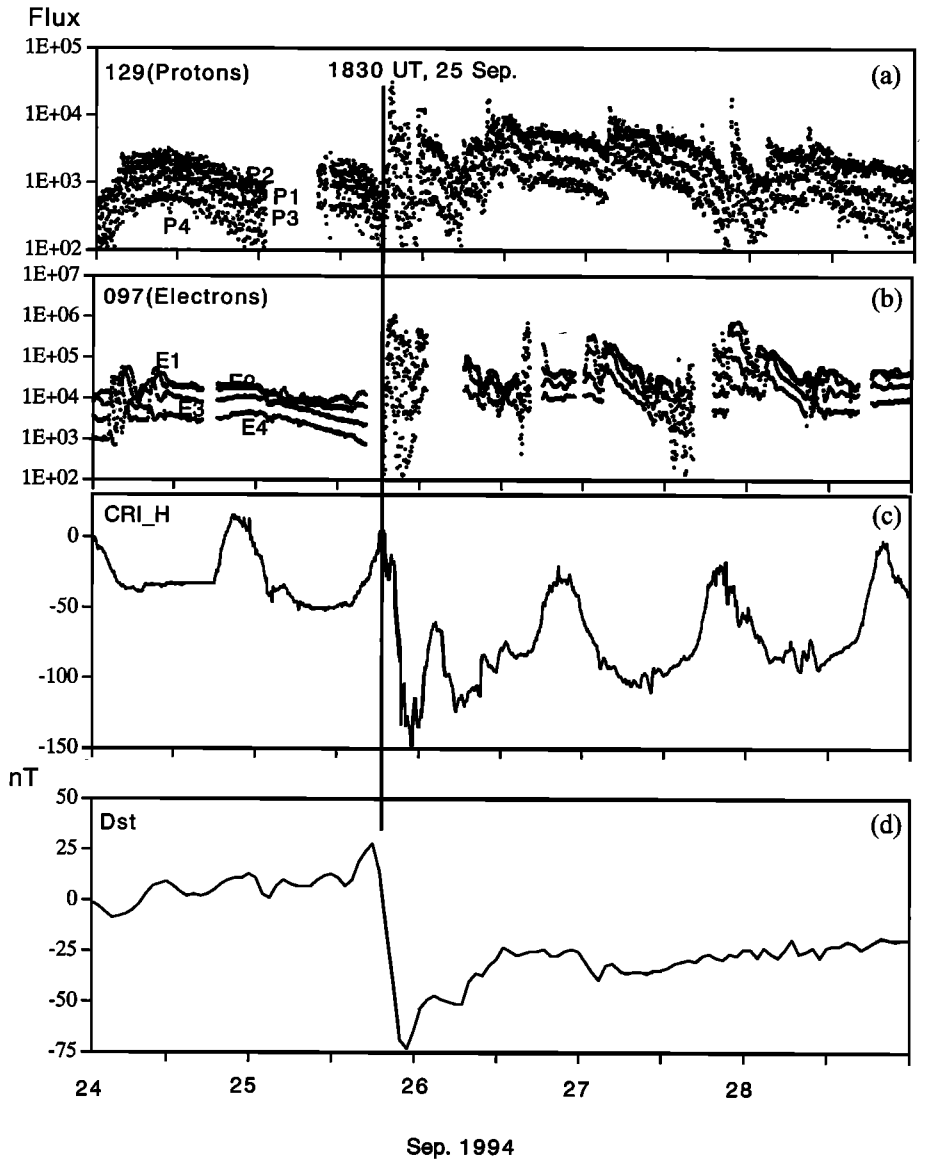

Figure 1. A 5-day plot of (a) the energetic proton flux ($cm^{-2}\ s^{-1}\ sr^{-1}$; P1: 75–88 keV, P2: 88–106 keV, P3: 106–129 keV, P4: 129–157 keV) from Los Alamos National Laboratory (LANL) geosynchronous satellite 1984-129, (b) the energetic electron flux ($cm^{-2}\ s^{-1}\ sr^{-1}$; E1: 30–45 keV, E2: 45–65 keV, E3: 65–95 keV, E4: 95–140 keV) from LANL geosynchronous satellite 1987-097, (c) the ground magnetometer H component at the dip equator (CRI), and (d) the *Dst* index. The geographic longitude of CRI was −157.5°, while geosynchronous satellite 1987-097 (1984-129) was at 103.7° (8.4°).

occurred at 1830 UT, while the Pi2 at 1904 UT will be discussed later.

The SuperDARN velocity data from these stations were plotted to obtain global line-of-sight velocity maps for the intervals of 1812:00–1824:00 UT (Plates 1a–1f), 1824:00–1836:00 UT (Plates 1g–1l), and 1836:00–1848:00 UT (Plates 1m–1r). Each interval group contains six maps, each of which was obtained every 120 s. The progression of time is depicted from left to right and from top to bottom. The convection velocities were mostly below 800 m s^{-1} in the SuperDARN field of view until 1824:00 UT. Thereafter, at 1824:00–1826:00 UT, the velocity enhancement commenced at the auroral region (~73°N) of a dusk sector. The convection increased to 1500 m s^{-1} in the next 2-min interval, 1826:00–1828:00 UT. The enhanced velocity region remained with less spatial movement and lasted for ~16 min until 1842:00–1844:00 UT, though it once decreased below 1000 m s^{-1} during the interval 1828:00–1830:00 UT. The velocity plots of the G and W radar overlapped at the dusk sector during the interval of convection enhancement. They were dominated by the toward-vector (southwestward) for the G radar and by the away-vector (northwestward) for the W radar. By merging these line-of-sight velocity vectors, the westward flow was dominated in the enhanced convection region at the dusk sector.

The ground station CRI was in the dayside sector of the dip equator, 0800 LT, during the particle injection. The enlarged plot shown in Figure 3 (1700–2000 UT) gives a close look at an injection onset together with the ground magnetometer data at the dip equator. Figure 3a shows energetic electron flux data of a geosynchronous satellite at the postmidnight sector. Figure

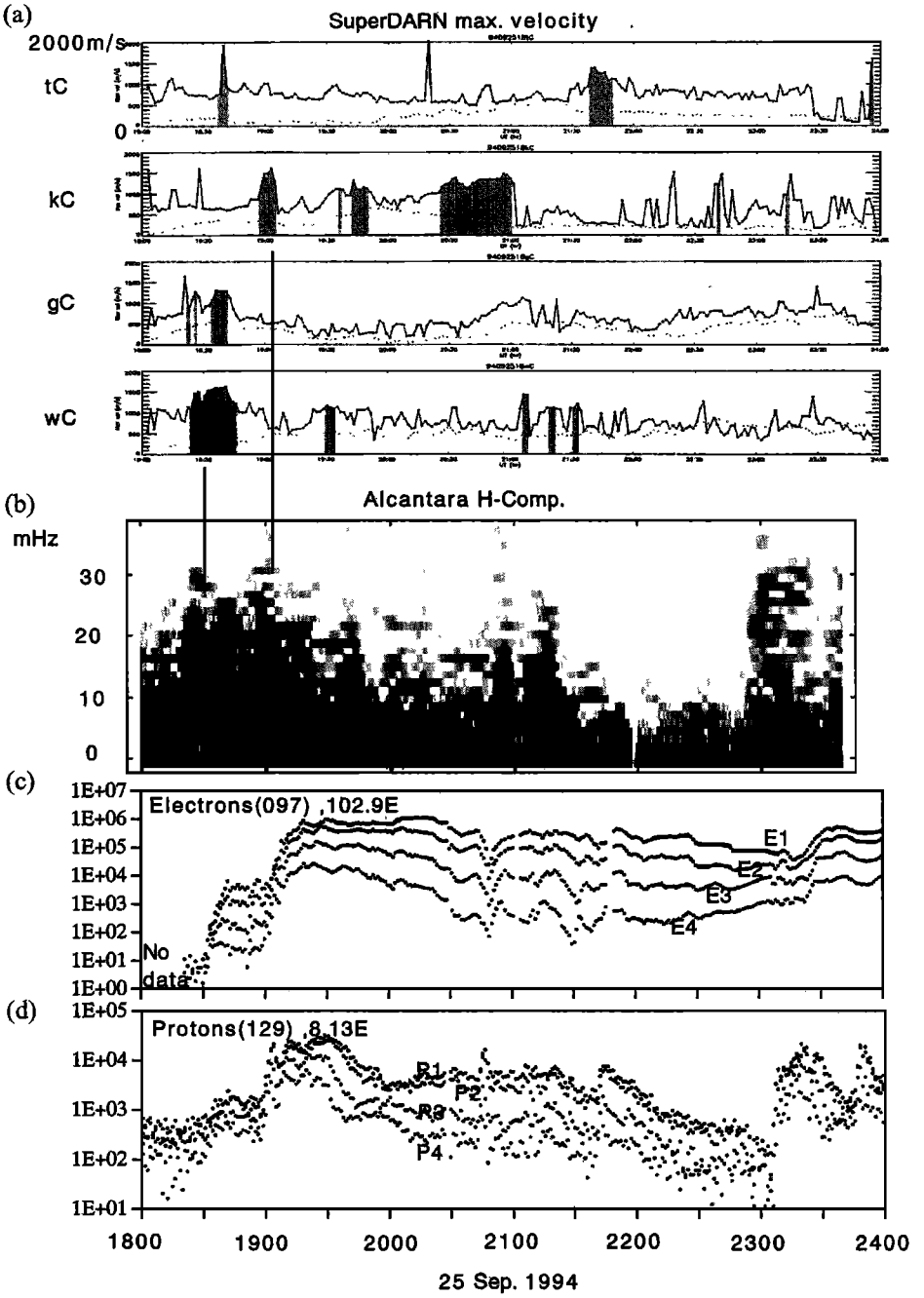

Figure 2. A stack plot of the September 25, 1994, event for the interval 1800–2400 UT: (a) SuperDARN maximum convection velocity (tC, Saskatoon; kC, Kapuskasing; gC, Goose Bay; wC, Stokkseyri), (b) power spectra of the ground magnetometer at ALC calculated by the fast Fourier transform (FFT) technique (256 data points; 3 s × 256 = 12.8 min interval, sliding by 1 min interval), (c) energetic electron flux (E1 through E4) from geosynchronous satellite 1987-097, and (d) energetic proton flux (P1 through P4) from geosynchronous satellite 1984-129. The timescale in the abscissa is the same for all plots. The vertical lines correspond to the onsets of the Pi2s (1830 and 1904 UT).

3b is ground magnetometer data of the H component from the dayside equator, CRI. Power spectra of the H component calculated by the fast Fourier transform (FFT) technique are in Figure 3c. The enhanced wave activities can be seen at the 8 mHz band; waveform was less clearly identified in the CRI magnetometer data, as the background fluctuations overlapped throughout the interval shown. It is worth noting that a concurrent change of the background fields, such as an equatorial counter electrojet, cannot be seen. To clarify the waveform signatures in FFT spectra observed at CRI, we show in Figure 3d a plot of the H and Z components of the low-latitude ground magnetometer at the premidnight sector (CNX; 11.2°N, 170.6° in geomagnetic coordinates; 18.8°N, 99.0° in geographic coordinates; 1945 LT sector at 1830 UT). Because of the data gap in the H component for the interval 1859–1905 UT, the FFT spectra were calculated by use of the Z compo-

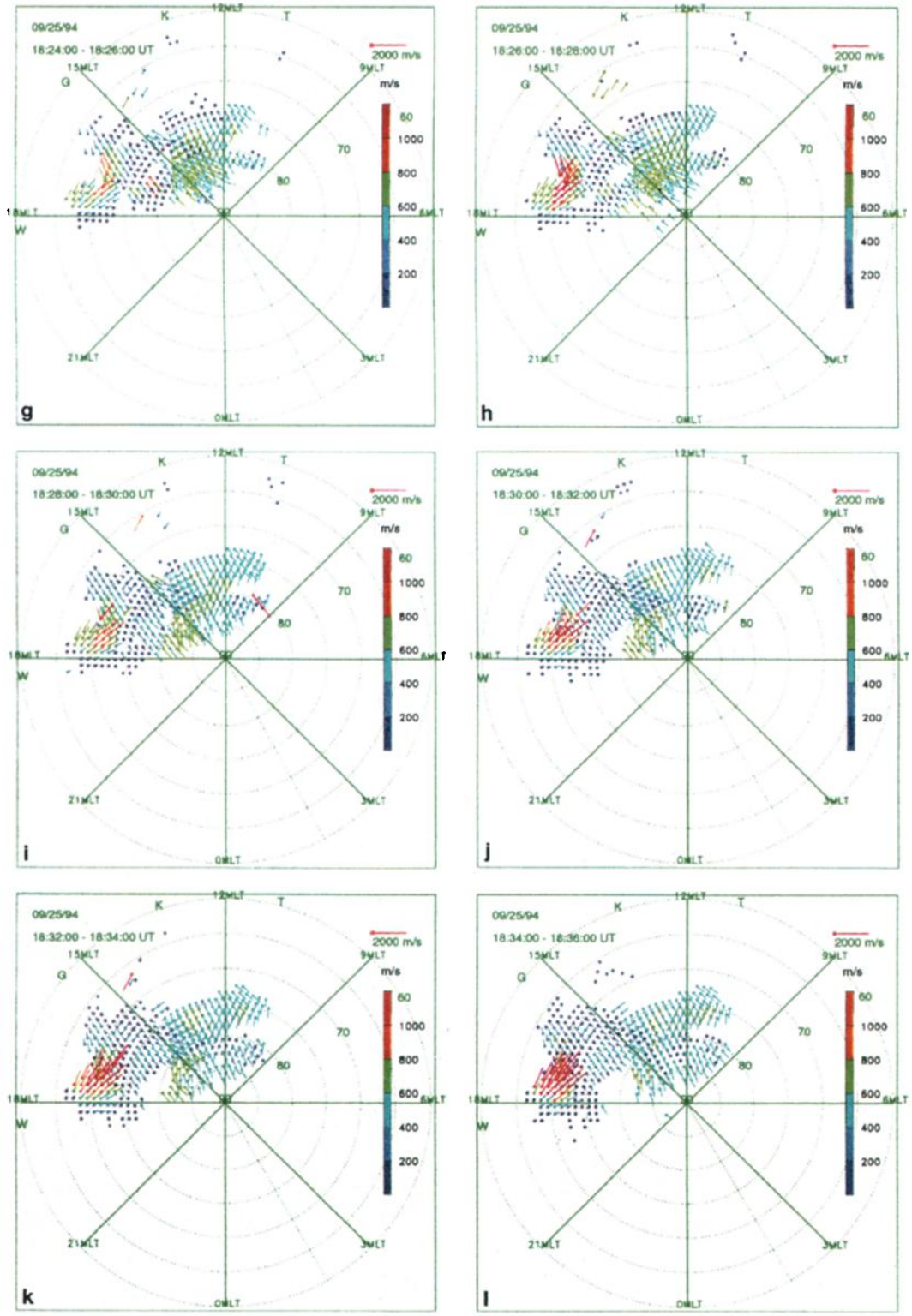

Plate 1. (continued)

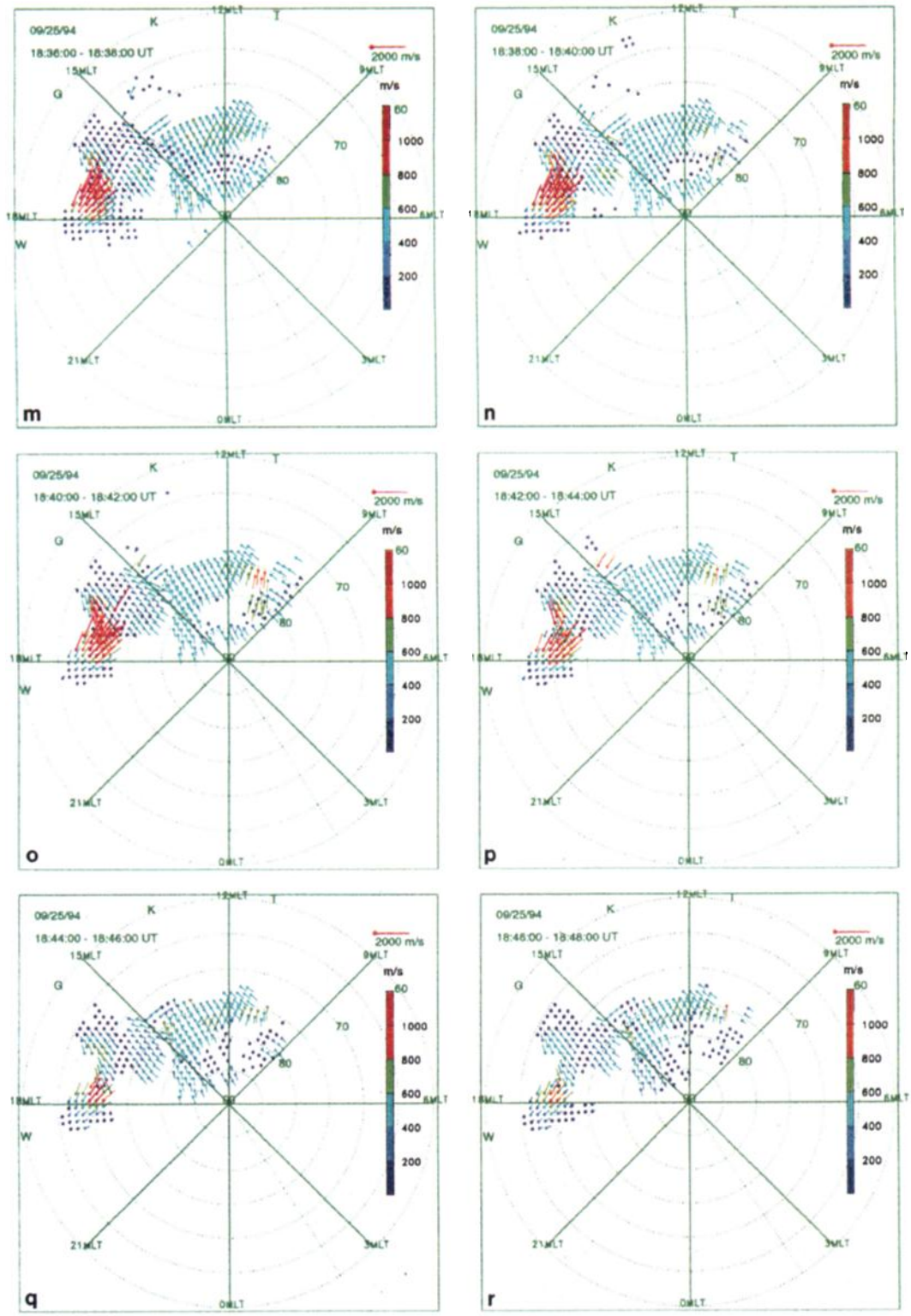

Plate 1. (continued)

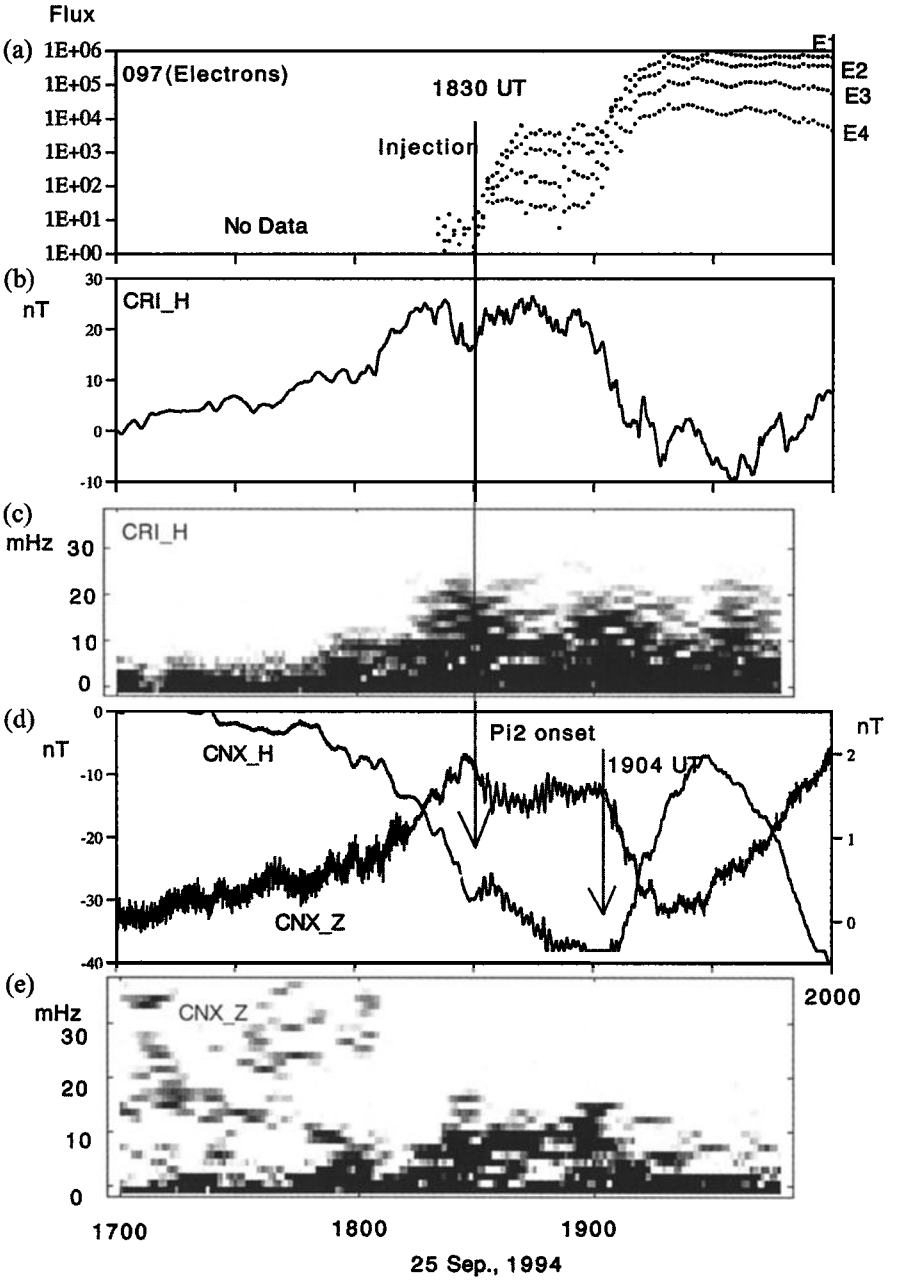

Figure 3. Enlarged plot of the September 25, 1994, event for the interval 1700–2000 UT. Figure 3a depicts energetic electron flux ($cm^{-2}\ s^{-1}\ sr^{-1}$; E1: 30–45 keV, E2: 45–65 keV, E3: 65–95 keV, E4: 95–140 keV) from the LANL 1987-097 satellite at the midnight sector (1830 UT = 0122 LT). The vertical bar in Figure 3a indicates the simultaneous onset of dispersionless electron injection and Pi2 pulsation at 1830 UT. Figures 3b and 3c demonstrate a plot of the magnetometer H component for CRI at the dayside sector (1830 UT = 0800 LT) and a profile of the dynamic power spectra calculated by the FFT technique (256 data points; 3 s × 256 = 12.8 min interval, sliding by 1 min interval), respectively. Figures 3d and 3e depict a plot of the H and Z components (the amplitude scale is to the left (right) for the H (Z) component) and power spectra of the Z component of the ground station CNX in the midnight sector (1830 UT = 0106 LT). In the Z component a contamination of higher-frequency noises can be seen before 1815 UT. The vertical bar at 1904 UT indicates a second Pi2 onset (see text).

nent and are demonstrated in Figure 3e. We could demonstrate a clear waveform of Pi2 pulsation for both the H and Z components (Figure 3d) in the 8 mHz band (Figure 3e) in the premidnight sector. From the CNX plot the onset of the first Pi2 can be better identified at 1830 UT, as marked by the vertical bar. It is apparent that the first Pi2 onset was delayed by 4–6 min with respect to the SuperDARN convection flow burst, where the flow increased in the dusk sector from 800 to 1500 m s^{-1} at the 1824:00–1826:00 UT interval.

2.2. April 2, 1994, Event

Energetic particle injection occurred at 0033 UT of April 2, 1994, at the midnight sector (Figure 4). The ground magnetometer stations at the dip equator were not in the dayside

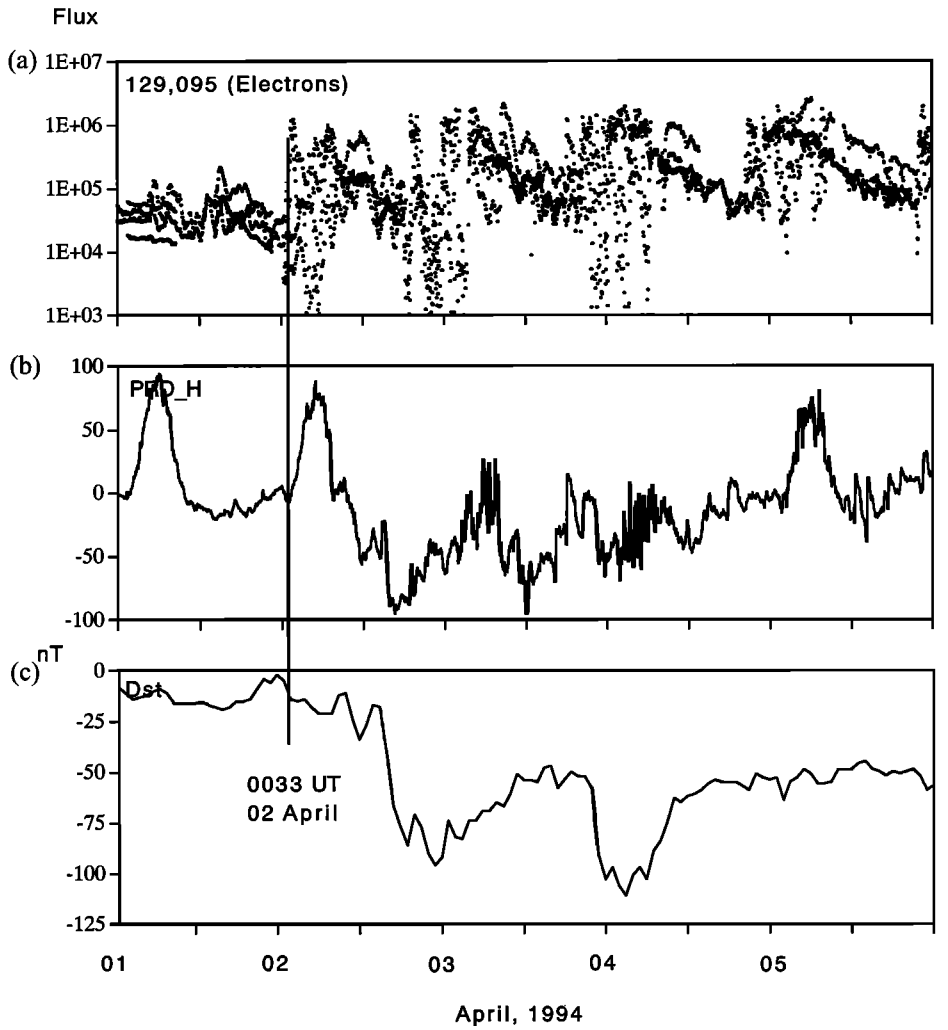

Figure 4. (a) A superimposed plot from two electron channels (cm^{-2} s^{-1} sr^{-1}; E1: 30–45 keV, E2: 45–65 keV) from LANL geosynchronous satellites 1984-129 and 1990-095, (b) the ground magnetometer H component at the dip equator (PRD), and (c) the *Dst* index. The plot covers the 5-day interval of April 1–5, 1994.

sector for the April event. In Figure 4 the H component plot from the ground magnetometer station PRD (Peradenia: 7.28°N, 80.64° in geographic coordinates; −0.10°, 152.30° in geomagnetic coordinates) is shown. A development of the *Dst* index was seen to occur as for the previous event, but the *Dst* developed gradually during the first 12 hours after the injection. In association with the particle injection, a SuperDARN flow burst was seen to occur at the dusk sector of the auroral region. To illustrate this event, we present in Figures 5a–5d a maximum convection velocity plot from three SuperDARN radars, power spectra of the ground magnetometer data from ALC (Alcantara: 2.34°S, −44.41° in geographic coordinates; 0.67°N, 29.33 in geomagnetic coordinates), and energetic electron flux from LANL satellites (1984-129 at 8.37° in geographic longitudes, 1990-095 at −37.6° in geophysical longitudes) at the midnight sector. Again, a multiple onset of the Pi2 can be seen in association with the corresponding injections in the dynamic power spectra. We will examine the onset of the first Pi2 event by use of an enlarged plot in Figure 6. In Figure 6 a Pi2 onset is less clearly identified in the ALC plot, as it is embedded in a sharp decrease of the background field, while the onset is estimated to be 0033 UT from the PRD plot, as marked by the vertical bar. One minute later, a dispersionless electron injection was detected by the geosynchronous satellites at the 0108 LT sector (Figure 6a) and at the 2207 LT sector (Figure 6b).

A flow burst of the ionospheric convection was detected as well by SuperDARN radars (Saskatoon (T), Kapuskasing (K)), as can be seen in the SuperDARN maximum velocity plot in Figure 5a. For the Kapuskasing data a transient increase seemed to start at 0020 UT, and maximum velocity of 1200 m s^{-1} was observed at 0025 UT. The velocity increased from 500 to 1200 m s^{-1} in 5 min, while for the Saskatoon data, the maximum velocity, ~1200 m s^{-1}, was obtained thereafter at 0030 UT.

The SuperDARN velocity data from Saskatoon (T), Kapuskasing (K), and Goose Bay (G) were plotted to obtain the global line-of-sight velocity map for the intervals of 0018:00–0026:00 UT (Plates 2a–2d), 0026:00–0034:00 UT (Plates 2e–2h), and 0034:00–0040:00 UT (Plates 2i–2k). Echoes were returned mostly from the afternoon sector. The maps in each interval group were obtained every 120 s. The progression of time is depicted from left to right and from top to bottom. The convection velocities were mostly below 600 m s^{-1} until

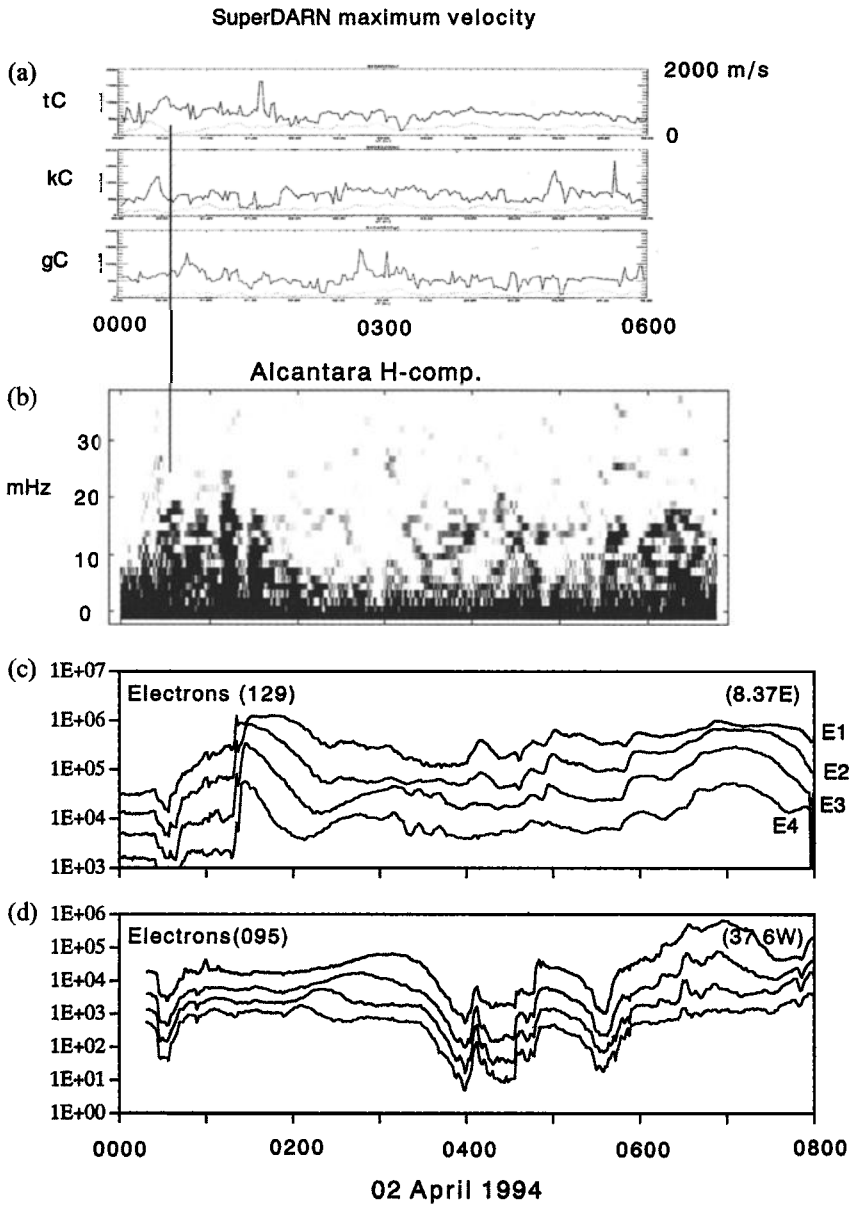

Figure 5. A stack plot of the April 2, 1994, event for the interval 0000–0800 UT: (a) SuperDARN maximum convection velocity plots (tC, Saskatoon; kC, Kapuskasing; gC, Goose Bay), (b) power spectra of ground magnetometer at ALC calculated by the FFT technique (256 data points; 3 s × 256 = 12.8 min interval, sliding by 1 min interval) (0000–0700 UT), and energetic electron flux (cm^{-2} s^{-1} sr^{-1}; E1: 30–45 keV, E2: 45–65 keV, E3: 65–95 keV, E4: 95–140 keV) from geosynchronous satellites (c) 1984-129 (8.4° in geographic longitudes) and (d) 1990-095 (−37.5° in geographic longitudes). The timescale in the abscissa is the same for all plots. The vertical line corresponds to the onset of the first Pi2.

0022:00 UT. Thereafter, at 0022:00–0024:00 UT, the velocity enhancement commenced at a latitude of ~70°N of a dusk sector. The convection increased to above 1000 m s^{-1} in the next 2-min interval, 0024:00–0026:00 UT. The flow burst remained with less spatial movement as for the previous case and lasted for ~14 min until 0036:00–0038:00 UT. Velocity plots from the T and K radars overlapped in the dusk sector, which enabled estimation of the flow vector by merging the line-of-sight velocity vectors from these radar stations. The enhanced velocities were away (northwestward) for the K radar throughout the region, while for the T radar they were toward (southwestward) below ~74°N and away (northeastward) above ~74°N (see the 0026:00–0028:00 UT interval). From this velocity pattern, westward (eastward) convection may prevail in the lower (higher) latitude portion. Accordingly, a focus of the clockwise convection vortex can be seen at ~71°N.

As a result, we suggest that the ionospheric convection enhancement occurred in the dusk sector in the same manner as the September 25, 1994, event. The time lag of the Pi2 onset was, however, 9–11 min for the April event. The time lag shown was not based on a statistical study but on a case study.

3. Summary and Discussions

The enhancement of the westward convection took place in the dusk sector of the auroral zone prior to the Pi2 onset. The

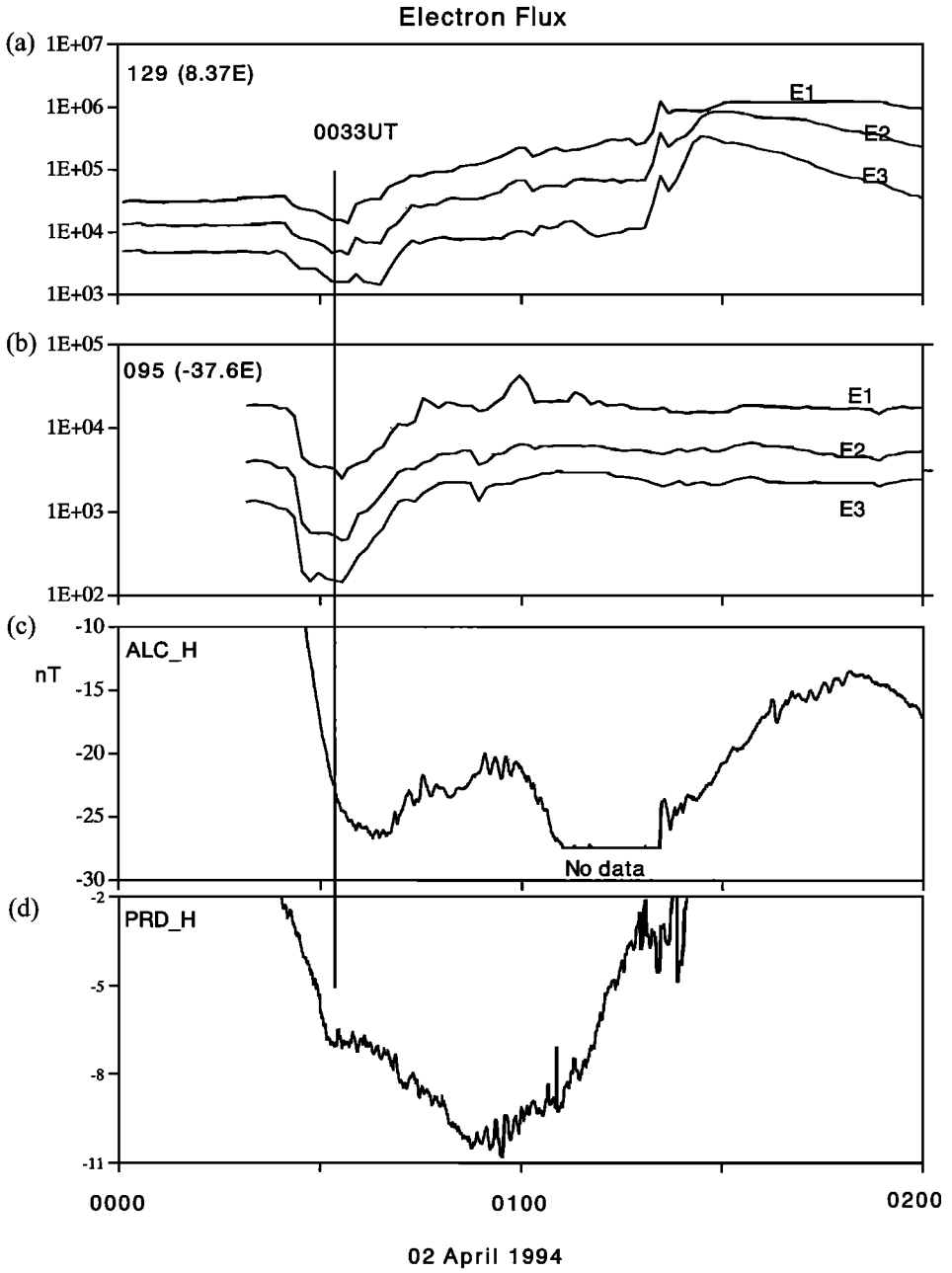

Figure 6. Enlarged plot for the interval 0000–0200 UT, April 2, 1994. Figures 6a and 6b depicts energetic electron flux ($cm^{-2}\ s^{-1}\ sr^{-1}$; E1: 30–45 keV, E2: 45–65 keV, E3: 65–95 keV) at the midnight sector from the LANL 1984-129 and 1990-095 satellites. Figures 6c and 6d demonstrate a plot of the magnetometer H component for ALC at the midnight sector (0033 UT = 2135 LT) and for PRD at the dawn sector (0033 UT = 0556 LT). The vertical bar in Figure 6a indicates the Pi2 onset at 0033 UT.

time delay (4–11 min) of the Pi2 onset with respect to the onset of the convection enhancement is evident even if the delay of the Pi2 transmission down to the ground (~1 min) is taken into account. Accordingly, we can suggest that the westward convection enhancement occurs in the auroral region several minutes prior to the particle injection, preceding the associated Pi2 onset on the order of minutes.

There have been a number of observations of high-speed flows in the dusk local time sector of the subauroral region [e.g., *Anderson et al.*, 1991, 1993; *Freeman et al.*, 1992; *Shand et al.*, 1998; *Spiro et al.*, 1979]. Because these high-speed flows, referred to as substorm-associated radar auroral surge (SARAS) or subauroral ion drift (SAID), were suggested to occur well after the substorm onset, the SARAS/SAID were interpreted as indicating a magnetospheric and ionospheric response that would be established in the Earth magnetosphere after development of the substorm expansion [e.g., *Freeman et al.*, 1992; *Anderson et al.*, 1993]. Owing to the different onset timing in the substorm phase, we suggest that the SuperDARN convection enhancement examined in this report may not belong to the type classified as SARAS/SAID.

The drift of the aurora fragment was examined by analyzing the all-sky image [*Nakamura and Oguti*, 1987]. The drift was westward in the dusk sector of the auroral zone; it can be

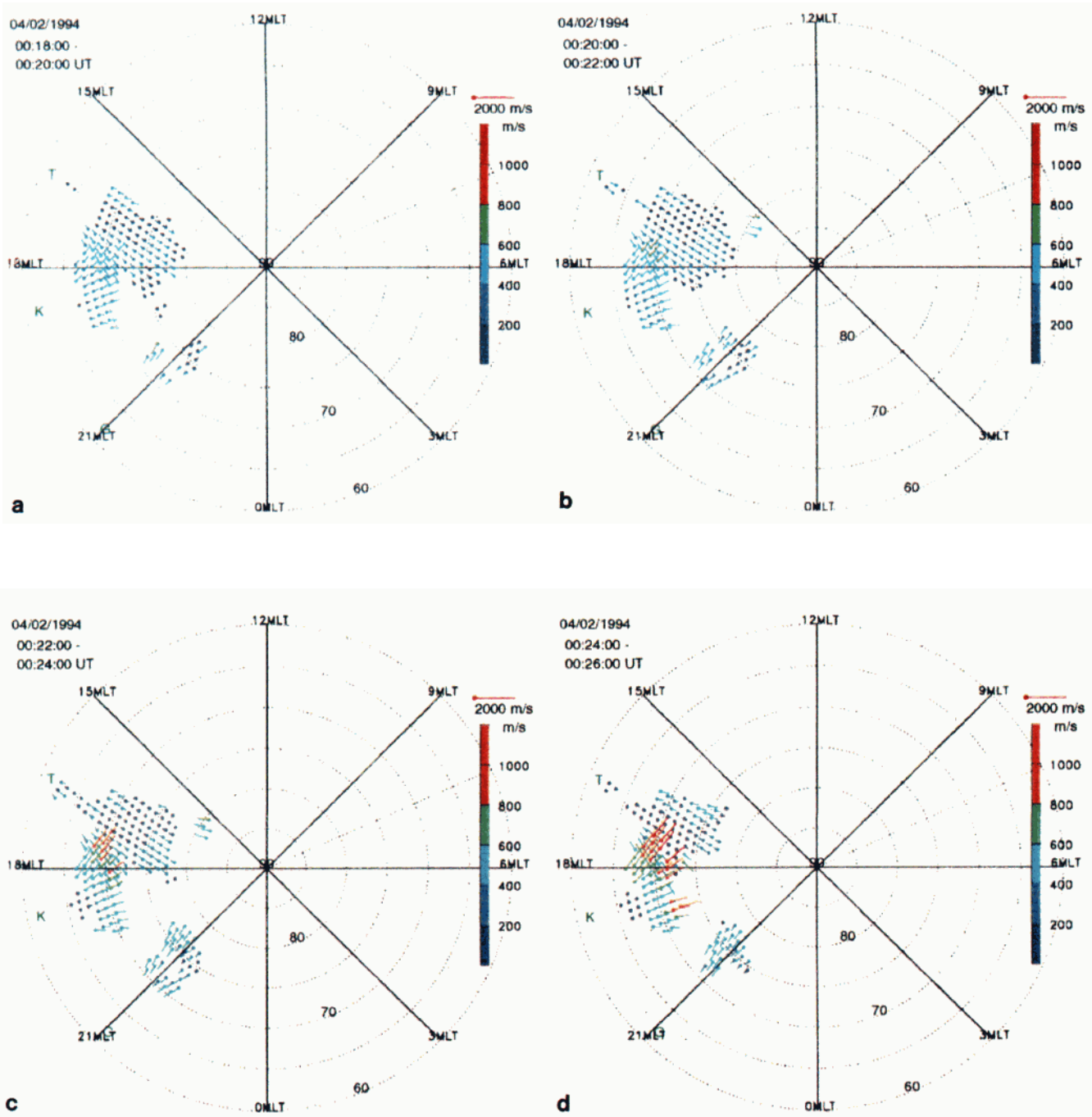

Plate 2. Plot of the averaged line-of-sight velocity values obtained from the SuperDARN radars on April 2, 1994: (a) 0018:00–0020:00 UT, (b) 0020:00–0022:00 UT, (c) 0022:00–0024:00 UT, (d) 0024:00–0026:00 UT, (e) 0026:00–0028:00 UT, (f) 0028:00–0030:00 UT, (g) 0030:00–0032:00 UT, (h) 0032:00–0034:00 UT; (i) 0034:00–0036:00 UT, (j) 0036:00–0038:00 UT, (k) 0038:00–0040:00 UT. The longitude positions (in geomagnetic coordinates) of the contributing radars are indicated by the letters along the 60°N contour; T, Saskatoon; K, Kapuskasing; G, Goose Bay.

attributed to dawn-to-dusk electric fields in the nightside magnetosphere. The velocities were found to range from 50 to 2000 m s^{-1}. In particular, the drift velocities were enhanced during substorms, and the onset time advanced toward the higher latitudes [*Nakamura and Oguti*, 1987; *Nakamura et al.*, 1988]. The present result is consistent with a westward convection enhancement as observed by the drift of aurora fragment in the all-sky image.

Possible interpretation of this event is that the convection enhancement as observed by SuperDARN was an ionospheric signature of the enhanced plasma convection taking place in the duskside magnetosphere prior to the onset of the energetic particle injection and Pi2. As the substorm expansion commences with the burst-like signatures of the plasmas, such as aurora breakup and energetic particle injection, the flow burst of the SuperDARN convection reported in this study could be

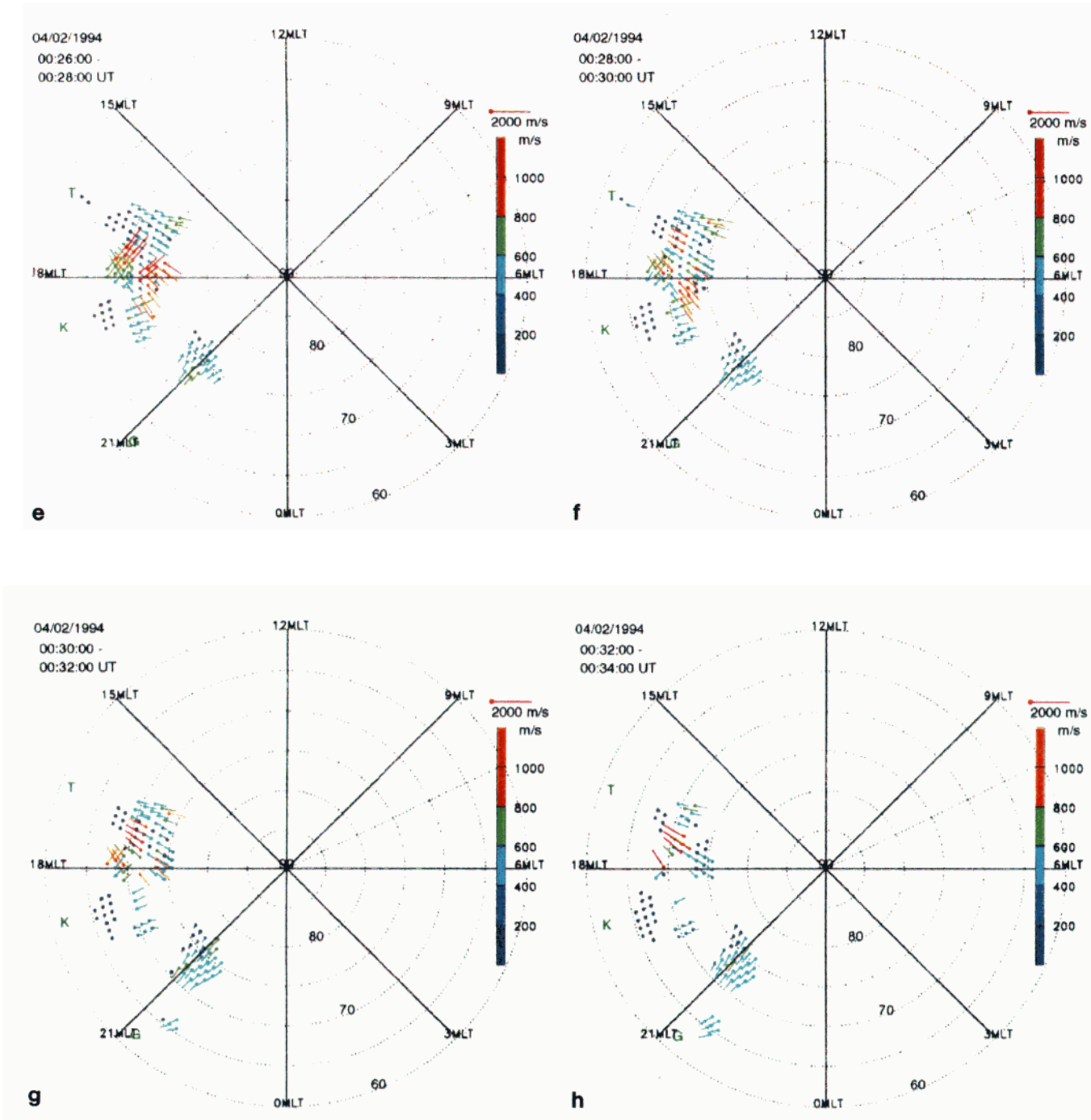

Plate 2. (continued)

the earliest onset signature of the substorm. Although the interplanetary magnetic field (IMF) data were not available for these intervals examined, the expansion of the polar cap may trigger such a flow burst during the transfer of the open magnetic flux into the polar cap. Indeed, a flow burst associated with the second Pi2 onset (1904 UT) of September 25, 1994, was recorded at the poleward portion of the dayside auroral region by the K radar (~77°N, 1500 MLT) (not shown). The flow burst seemed to occur a few minutes prior to the Pi2 onset, though the Pi2 onset was less clearly identified, as it overlapped the sharp decrease of the background field change (see Figure 1). It has been suggested that the Pi2 onset could be interpreted as indicating a transient response of the magnetic fields in the inner magnetosphere to the increased plasma pressures brought by the fresh particles from the tail. These particles may be supplied along the field lines [*Saka et al.*, 2000a]. If we assume that the earthward field-aligned flow of the plasmas was of the order of 500 km s^{-1} in the tail magnetosphere [*Paterson et al.*, 1998] and that the time delay of the order of ~5 min can be regarded as a traveling time of the plasmas, those plasmas would have originated from a region 30 R_E tailward of the Earth. This location is suggested as a potential site of the magnetic reconnection [*Nagai et al.*, 1998; *Baker et al.*, 1999]. Another interpretation of the Pi2 and flow

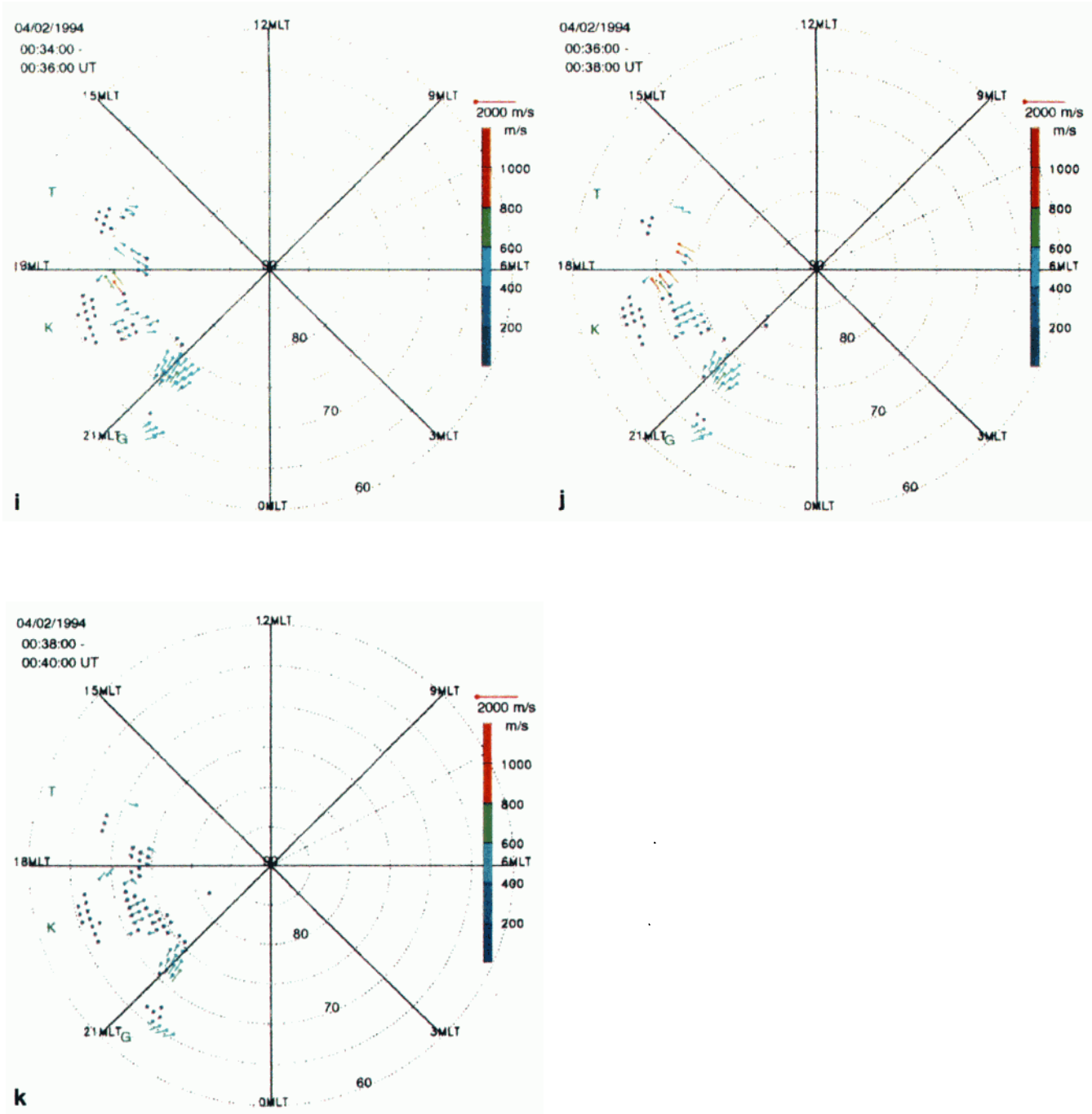

Plate 2. (continued)

burst correlation observed is that the time delay is a transit time of the plasmas traveling from the reconnection site to the inner magnetosphere.

At the equator the ring current effect that developed after the injection was significant, but only a pulsation signature was detected at the moment of particle injection. A direct penetration of the injection disturbances at the substorm onset was less significant at the dip equator, as the Earth shielding system seemed to operate properly. As a result, the convection enhancement associated with the fresh particle injection in the midnight magnetosphere was confined more or less in the auroral zone. This is in contrast to the IMF effect examined in our previous report [*Saka et al.*, 2000b], in which the negative impulse referred to as equatorial counter electrojet appeared at the dayside dip equator coincident with the IMF negative B_z impulse in the solar wind.

Acknowledgments. Thanks are due to the Meteor office at Christmas Island, Republic of Kiribati, to V. Wang at CNX, Thailand, and to B. S. B. Karunaratne (U. Peradenia) at PRD, Sri Lanka, for magnetometer operation. Thanks are also to T. Oguti for informative discussions. The LANL energetic particle data were provided through G. D. Reeves. The *Dst* index was provided through WDC-C2 for geomagnetism, Kyoto University. We thank one of the referees for valuable comments and suggestions.

Hiroshi Matsumoto thanks M. Lester and T. J. Rosenberg for their assistance in evaluating this paper.

References

Akasofu, S.-I., and C.-I. Meng, Low latitude negative bays, *J. Atmos. Terr. Phys.*, *30*, 227–241, 1968.

Anderson, P. C., R. A. Heelis, and W. B. Hanson, The ionospheric signatures of rapid subauroral ion drifts, *J. Geophys. Res.*, *96*, 5785–5792, 1991.

Anderson, P. C., W. B. Hanson, R. A. Heelis, J. D. Craven, D. N. Baker, and L. A. Frank, A proposed production model of rapid subauroral ion drifts and their relationship to substorm evolution, *J. Geophys. Res.*, *98*, 6069–6078, 1993.

Baker, D. N., T. I. Pulkkinen, J. Buchner, and A. J. Klimas, Substorms: A global instability of the magnetosphere-ionosphere system, *J. Geophys. Res.*, *104*, 14,601–14,611, 1999.

Blanc, M., and A. D. Richmond, The ionospheric disturbance dynamo, *J. Geophys. Res.*, *85*, 1669–1686, 1980.

Freeman, M. P., D. J. Southwood, M. Lester, T. K. Yeoman, and G. D. Reeves, Substorm-associated radar auroral surges, *J. Geophys. Res.*, *97*, 12,173–12,185, 1992.

Jacobs, J. A., *Geomagnetic Micropulsation*, Springer-Verlag, New York, 1970.

Lanzerotti, L. J., and H. Fukunishi, Modes of hydromagnetic waves in the magnetosphere, *Rev. Geophys.*, *12*, 724–729, 1974.

Liou, K., C.-I. Meng, T. Y. Lui, and P. T. Newell, On relative timing in substorm onset signatures, *J. Geophys. Res.*, *104*, 22,807–22,817, 1999.

McPherron, R. L., Substorm associated micropulsations at synchronous orbit, *J. Geomagn. Geoelectr.*, *32*(2), SII57–SII68, 1980.

Nagai, T., et al., Structure and dynamics of magnetic reconnection for substorm onsets with Geotail observations, *J. Geophys. Res.*, *103*, 4419–4440, 1998.

Nakamura, R., and T. Oguti, Drifts of auroral structures and magnetospheric electric fields, *J. Geophys. Res.*, *92*, 11,241–11,247, 1987.

Nakamura, R., T. Yamamoto, and T. Oguti, Enhancements in auroral drift velocity in the dusk sector associated with a small substorm in the midnight sector, *J. Geomagn. Geoelectr.*, *40*, 409–422, 1988.

Nishida, A., *Geomagnetic Diagnosis of the Magnetosphere*, Springer-Verlag, New York, 1978.

Olson, J. V., Pi2 pulsations and substorm onset: A review, *J. Geophys. Res.*, *104*, 17,499–17,520, 1999.

Onwumechili, A., K. Kawasaki, and S.-I. Akasofu, Relationships between the equatorial electrojet and polar magnetic variations, *Planet. Space Sci.*, *21*, 1–16, 1973.

Paterson, W. R., L. A. Frank, S. Kokubun, and T. Yamamoto, Geotail survey of ion flow in the plasma sheet: Observations between 10 and 50 R_e, *J. Geophys. Res.*, *103*, 11,811–11,825, 1998.

Senior, C., and M. Blanc, On the control of magnetospheric convection by the spatial distribution of ionospheric conductivities, *J. Geophys. Res.*, *89*, 261–284, 1984.

Saito, T., Geomagnetic micropulsations, *Space Sci. Rev.*, *10*, 319–412, 1969.

Saka, O., H. Akaki, G. D. Reeves, and D. N. Baker, Magnetic fields and particle signatures in the vicinity of nightside geosynchronous altitudes in the first one-minute interval of Pi2 onset: A case study, *J. Atmos. Sol. Terr. Phys.*, *62*, 17–30, 2000a.

Saka, O., T. Kitamura, H. Tachihara, M. Shinohara, N. B. Trivedi, N. Sato, J. M. Ruohoniemi, and R. A. Greenwald, Simultaneous transients in the auroral zone and in the equator as observed with SuperDARN and magnetometers: A correlation with equatorial counter electrojet (CEJ) event, *Adv. Polar Upper Atmos. Res.*, *14*, 45–54, 2000b.

Sakurai, T., and R. L. McPherron, Satellite observations of Pi2 activity at synchronous orbit, *J. Geophys. Res.*, *88*, 7015–7027, 1983.

Shand, B. A., M. Leser, and T. K. Yeoman, Substorm associated radar auroral surges: A statistical study and possible generation model, *Ann. Geophys.*, *16*, 441–449, 1998.

Southwood, D. J., and W. F. Stuart, Pulsations at the substorm onset, in *Dynamics of the Magnetosphere*, edited by S. I. Akasofu, pp. 341–360, D. Reidel, Norwell, Mass., 1980.

Spiro, R. W., R. A. Heelis, and W. B. Hanson, Rapid subauroral ion drift observed by Atmosphere Explorer C, *Geophys. Res. Lett.*, *6*, 657–660, 1979.

Yeoman, T. K., M. P. Freeman, G. D. Reeves, M. Lester, and D. Orr, A comparison of midlatitude Pi2 pulsations and geostationary orbit particle injections as substorm indicators, *J. Geophys. Res.*, *99*, 4085–4093, 1994.

R. A. Greenwald and J. M. Ruohoniemi, Applied Physics Laboratory, Johns Hopkins University, Laurel, MD 21218.

T. Kitamura, M. Shinohara, and H. Tachihara, Department of Earth and Planetary Sciences, Kyushu University, Fukuoka, Japan.

O. Saka, Department of Physics, Kurume National College of Technology, 1232 Komorino, Kurume, Fukuoka 830-8555, Japan. (saka@ges.kurume-nct.ac.jp)

N. Sato, National Institute of Polar Research, Tokyo, Japan.

N. B. Trivedi, Instituto Nacional de Pesquisas Espacias, Sao Jose dos Campos, Spain.

(Received October 19, 2000; revised April 11, 2001;
accepted June 18, 2001.)